PSF Fitting of WFCAM Data: Astrometry

Document number: VDF-TRE-IOA-00016-0004

Dafydd Wyn Evans, IoA

10 December 2004

1 Introduction

As stated in the previous PSF report ([Evans 2004]), it is intended that the development of PSF fitting within the WFCAM project be carried out in 3 phases. This report deals with Phase 2: a list-driven analysis with positional updating – this is as in Phase 1, but the positions are iterated around the given position to determine the best PSF fit, yielding both photometry and astrometry.

A good paper to read on this topic is [Anderson & King 2000] and a number of ideas are used from it, especially the use of the effective PSF.

2 The simulations carried out

The source data used in these tests were the same simulations as generated in [Evans 2003] and used for the previous PSF report. However, only two sets of simulations were used in these tests:

1. Interleaved data, with all four elements of the interleaved images generated with the same seeing ($0.6''$).
2. Non-interleaved data with the same total integration time as above.

The simulations were carried out down to J=22.2, so that some of the effect of undetected faint stars could also be accounted for (the detection limit is about J=20 [Irwin 2003]).

3 Description of general method used

The methodology used is fairly simple with the primary assumptions that:

1. All stellar positions down to a limiting magnitude are known.
2. The PSF for each star is known.

After a suitably binned PSF is generated for each detected star, a linear least-squares solution is applied to determine the flux level for these stars.

Using a list of detected stars (generated by another part of the pipeline), each star is processed in turn. A cutout is made around the star from the image data. Then, correctly sampled PSFs are generated for each star within the cutout that might affect the flux levels. The initial linear least-squares solution is generated from this subset of the data and using these PSFs.

The PSFs for the fitting were generated by bilinearly interpolating an oversampled PSF which was calculated using the data from the whole image. It was found very early on that using a simple scheme where the required PSFs were calculated using the nearest neighbour values from an oversampled PSF was not sufficient, even though the PSFs generated looked reasonable by eye. This was necessary, not

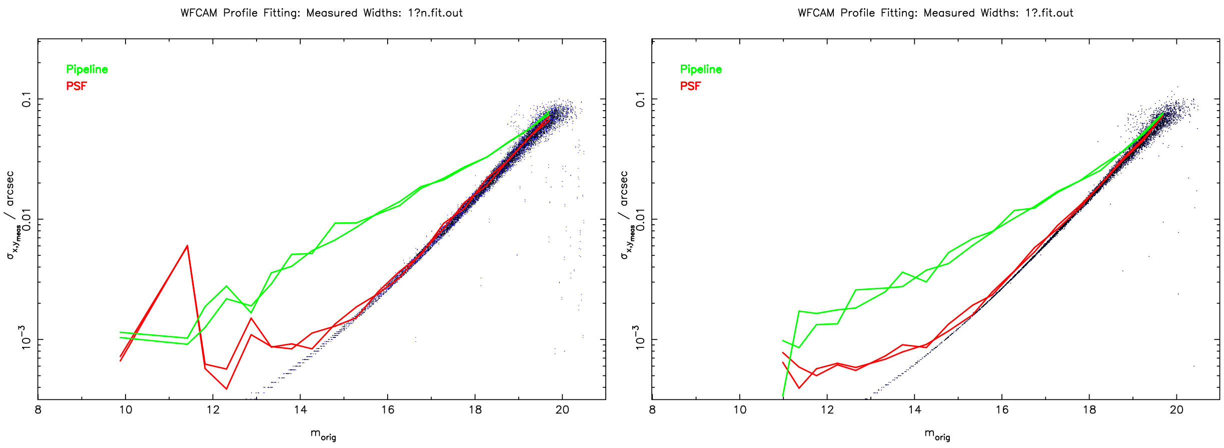

Figure 1: This plot shows the measured astrometric errors for the non-interleaved and interleaved data. The results for the standard pipeline astrometry is shown in green and that for the PSF fitting in red. The points show the formal errors estimated from the PSF fitting.

only for determining the PSFs of the primary star in the solution, but also for the PSFs of the perturbing stars. The background determination and solution weighting used was as described in the previous report.

After the initial photometric fit has been carried out, any contaminating images are removed from the cutout, leaving only the primary image, and a further fit is carried out to the data. This fit solves for the astrometry as well as for the photometry and is thus a non-linear one. The method chosen was the Levenberg-Marquardt method (see [Press *et al.* 1992]). This requires the partial differentials of the PSF with respect to X, Y and flux to be available. This is tabulated at the same time as the measurement of the PSF as described in the previous report and is computationally fast.

An alternative iterative grid method was tested where no differentials are used in the fit. Although similar results were found, the code was much slower.

Also tested was a restriction of the cutout to an aperture of radius twice the Gaussian sigma of the primary image. This had very little effect on the simulated data, but performed very poorly with real optical data, possibly due to the crowded field used. When real data is available from WFCAM more testing of this aspect will be carried out.

4 Analysis

For photometry, the addition of the non-linear fit does not improve the accuracy significantly and the results are as reported in the previous report.

As for photometry, the analysis of the results for the simulated data is carried out by comparing the true and fitted positions and measuring the widths of these distributions as a function of magnitude. This will give a good estimate of the accuracy of the method. This is shown in Figure 1 for the non-interleaved and interleaved data.

Also shown is the equivalent error estimation for the default astrometry generated by the standard CASU pipeline. In this idealized case, a substantial improvement in accuracies is obtained by using PSF fitting. Brighter than J= 18, the accuracies are a factor of between 2 and 5 times better.

These plots also show that the error estimation from the fitting process is in good agreement with that measured. Brighter than J=14–15, the measured accuracy levels off to 0.8 mas (1/500 pixel) for the non-interleaved data and 0.6 mas (1/300 pixel) for the interleaved data. This is probably due to limitations in the simulations (roundoff error *etc.*).

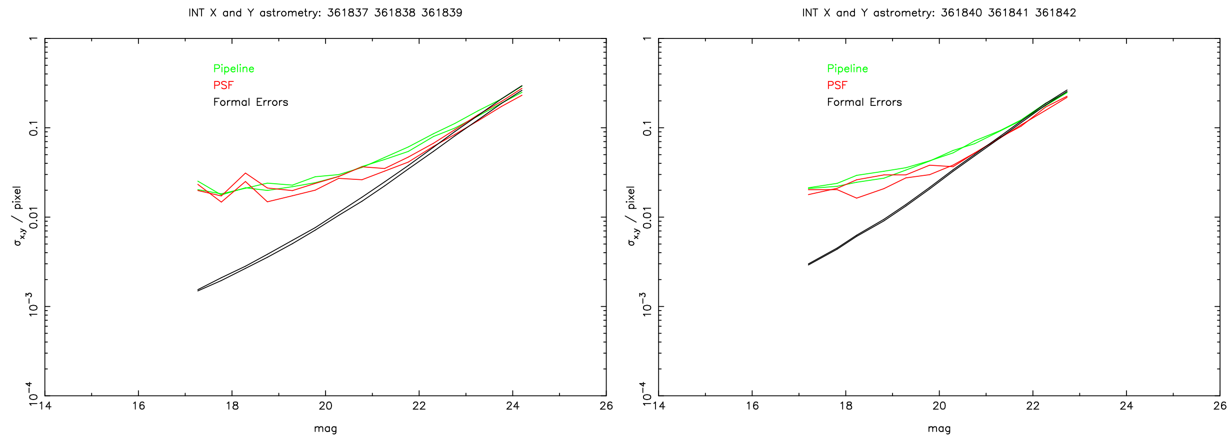

Figure 2: This plot shows the external errors for PSF (red) and standard pipeline (green) astrometry as a function of magnitude for data taken with the INT Wide Field Camera. The V band is on the left and i' on the right. Also shown are the average formal errors as a function of magnitude (black).

Fitting tests were carried out using two different PSF models. The default model used elliptical Moffat profiles as described in the previous report. The other model was an adaptive kernel one similar to that used in [Alard & Lupton 1998]. This model doesn't work quite as well as the one that uses elliptical Moffat profiles, but this might be expected since the simulations were carried out using Moffat profiles. Both methods will be considered for analysing the real data since the adaptive kernel method might have advantages if the PSF is spatially varying.

5 Speed of code

While carrying out these tests, the processing speed was noted in comparison with `imcore`, the standard pipeline programme for generating image parameters. On average, the determination of the PSF took about as long as `imcore` took to process the same file and the PSF fitting took about 2 to 3 times as long. It should be noted that a lot of diagnostic calculations are currently carried out in these programmes and no speed optimization has been attempted.

6 Use of PSF software on optical data

As in the previous report, INT Wide Field Camera data of the Wolf-Lundmark-Melotte (WLM) galaxy in the Local Group was used to test the software further. Three frames in each of the passbands Harris V and Sloan i' were analysed. By using 3 frames it is possible to determine the external astrometric and photometric errors for each frame by making the assumption that the width of the residuals in any comparison is equal to the quadrature sum of the external errors for each frame. With 3 frames it is possible to generate 3 sets of residuals and thus determine what the external errors are by solving the simultaneous equations. This also assumes that the errors are not correlated *ie.* they are independent. A weakness of this method is that the measurement of the widths of the distributions is quite noisy and the nature of the equations amplifies this. Sometimes solutions are not possible due to this noise. Often 2 frames taken in similar conditions is enough to determine the external errors by assuming that they are the same for both frames.

The results shown in Figure 2 indicate that the astrometric performance of PSF fitting is not very much better than that of the standard pipeline and certainly doesn't show the marked improvement possible demonstrated in the simulations (Figure 1). The limit of the accuracy achieved for this data is 7 mas (1/50 pixel).

Many explanations have been considered to explain what appears to be an additional, unaccounted for, systematic astrometric error:

1. A standard 6-parameter solution is not enough to match the data between the frames: quadratic terms were added but no improvement was observed in the accuracies. Similar results were found with radial terms up to the fourth power. As a test, a comparison was carried out with only offsets used for the matching and the accuracy limit rose to 30 mas (1/10 pixel).
2. The functional form of the solution used for the frame matching is inadequate: vector diagrams of the residuals were investigated and no systematic trends were visible. This would rule out astigmatism in the corrector as the source of the error.
3. Differential atmospheric refraction: this effect will mainly be in declination. Between the exposures, the airmass changes from 1.396 to 1.423 (44.25° to 45.35°). For the V passband, the ΔR between a B−V of 0.0 and 1.5 will be around $\sim$ 50 mas, thus the maximum size of effect is of order 1 mas and cannot explain the large errors.
4. Varying PSF across the frame: this is unlikely to be the source of the problem since the pipeline astrometry also seems to be similarly affected. Also the variation of the χ^2 statistic across the field seems to indicate that this is not a problem (see Section 7).
5. Problems with the autoguider: this would result in a shift or a distortion of the PSF, neither of which would explain the errors seen.
6. Crowded field: the exclusion of Extension 4 (the most crowded region) does not affect the results.
7. Chromaticity changes in the corrector: this is highly unlikely since the telescope is pointing in the same direction and the gravity vector has only changed by about a degree.
8. Pixel phase errors (see [Anderson & King 2000]): this should only affect undersampled data. However, it was checked and no effect was observed.
9. WFC field distortion[1]: a typical differential of the radial distortion is about 3000 mas over 750 pixels. Since the maximum shift between frames is about half a pixel this implies a systematic of about 2 mas. Additionally, the 6 parameter fit will remove a large part of this. Thus, the effect is too small.
10. CCD manufacturing inaccuracies: typical pixel tolerances for a CCD is about 0.5 μm. The WFC pixels are 13.5 μm. Although this is of the correct order of magnitude to explain the errors, the images are in the same locations on the CCDs to within a fraction of a pixel (maximum is half a pixel), thus these errors will be mostly mapped out since we are considering differential astrometry.

Both PSF models were tested and their performances were again very similar to each other.

7 The χ^2 distribution across the field of view

In order to see if the PSF is varying across the field of view the reduced χ^2 values are plotted as a function of position. These values are derived from the χ^2 values from the PSF fit and are divided by the number of degrees of freedom. Figure 3 shows the variation for one of the WLM exposures taken by the INT Wide Field Camera.

The dark region in the centre corresponds to the central parts of the galaxy and suffers from crowding effects. It is understandable that many of the images here will be affected by undetected (by the initial pipeline detection algorithm) images and thus the average PSF will not be a good fit to the data. Hence the χ^2 values for this part of the frame will be high.

Across the rest of the field of view there doesn't seem to be much variation of the reduced χ^2, indicating that the PSF does not vary.

[1]See `http://www.ast.cam.ac.uk/~wfcsur/technical/astrometry/`

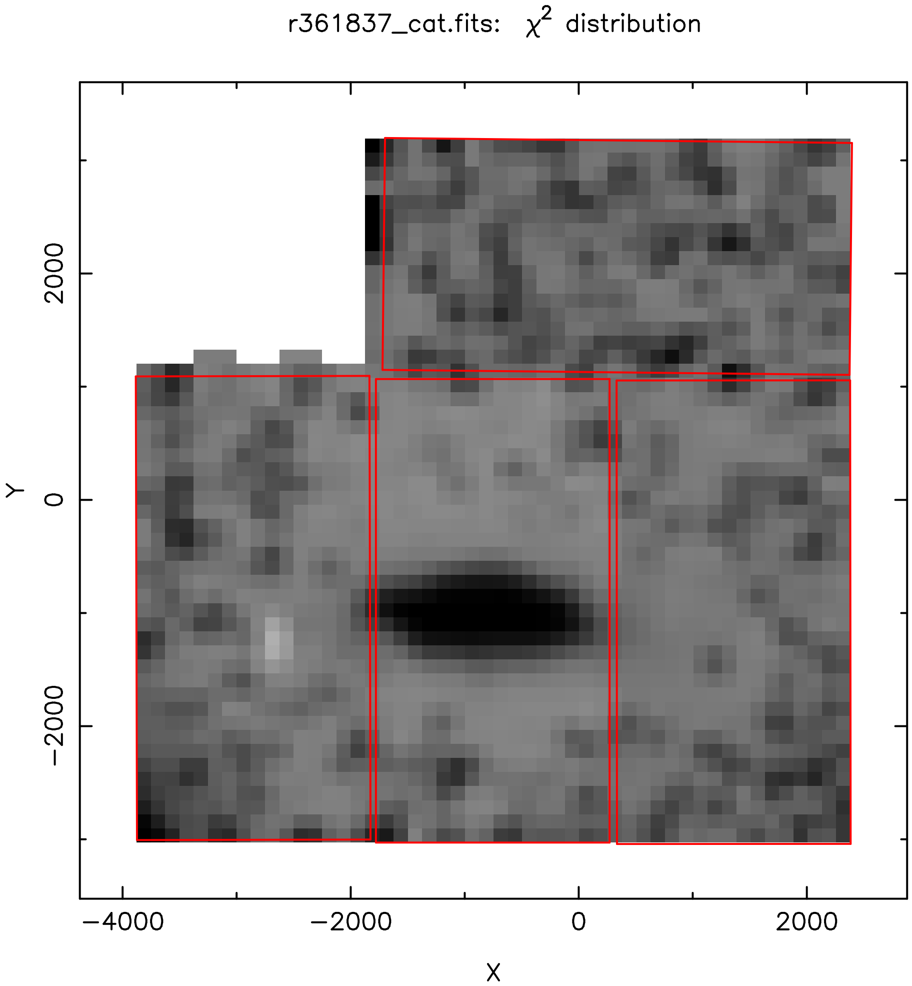

Figure 3: This plot shows the reduced χ^2 values across the field of view of the camera for exposure r361837. Midtone grey corresponds to a value of 1.0. A Hanning filter (33 Bartlett filter) has been applied to the data. The red outlines show the location of the 4 CCDs.

8 Conclusions

The simulations have shown that using PSF fitting can significantly improve astrometric accuracies. However, tests on optical data show that these improvements may not be realized.

What is now needed for the further testing of this software is real WFCAM data taken in good observing conditions.

A postscript version of this report can be found at
`http://www.ast.cam.ac.uk/~wfcam/docs/reports/psf2/psf2.ps`.

References

[Alard & Lupton 1998] Alard C., Lupton R.H., 1998, ApJ, 503, 325
'A Method for Optimal Image Subtraction'

[Anderson & King 2000] Anderson J., King I.R., 2000, PASP, 112, 1360
'Toward High-Precision Astrometry with WFPC2. I. Deriving an Accurate Point-Spread Function'

[Evans 2003] Evans D.W., 2003. Internal report
`http://www.ast.cam.ac.uk/~wfcam/docs/reports/interleaving/`
'Interleaving tests'

[Evans 2004] Evans D.W., 2004. Internal report
`http://www.ast.cam.ac.uk/~wfcam/docs/reports/psf/`
'PSF Fitting of WFCAM data'

[Irwin 2003] Irwin J.M., 2003. Internal report
`http://www.ast.cam.ac.uk/~wfcam/docs/reports/simul/#passbands`
'WFCAM simulations'

[Press *et al.* 1992] Press W.H., Teukolsky S.A., Vetterling W.T., Flannery B.P., 1992, Cambridge University Press
'Numerical Recipes in FORTRAN', 2nd edition, page 678